Available online at www.sciencedirect.com
SCIENCE DIRECT
Journal of Power Sources 158 (2006) 564–570
JOURNAL OF POWER SOURCES
www.elsevier.com/locate/jpowsour

Evaluation of GPE performances in lithium metal battery technology by means of simple polarization tests

L. Sannier [a], R. Bouchet [b,*], M. Rosso [c], J-M. Tarascon [a]

[a] *Laboratoire de Réactivité et Chimie des Solides, UPJV 33, Rue Saint Leu 80039 AMIENS Cedex, France*
[b] *Laboratoire MADIREL, Université de Provence, Centre Saint Jérôme, 13397 Marseille Cedex 20, France*
[c] *Laboratoire de la Physique de la Matière Condensée, Ecole Polytechnique, 91128 Palaiseau Cedex, France*

Received 29 April 2005; accepted 13 September 2005
Available online 16 November 2005

Abstract

Gel polymer electrolyte (GPE) membranes based on two polymers, a copolymer of poly(vinylidene fluoride–hexafluoropropylene) (PVdF–HFP), and the poly(ethylene oxide) (PEO), together with a plasticizer, the dibutylphtalate (DBP), were elaborated in two ways. Firstly, the polymers and the plasticizer were mixed together to obtain a single membrane. Secondly, a bi-layer separator membrane was made by adjunction, through lamination, of a DBP plasticized PVdF–HFP film and a homemade DBP–PEO thin film. We report here a protocol based on a simple galvanostatic polarization of Li/GPE/Li symmetric cells as a way to rapidly screen new viable membranes. Such a procedure enables to quickly discriminate separators by leading experiments that do no not exceed 1 week compared to hundreds of days needed with classical batteries. The validity of such an approach was confirmed by investigating the performances of the membranes in Li/GPE/$Li_4Ti_5O_{12}$ flat battery configuration. Besides, through this study we also highlighted the role of the macroscopic PEO–PVdF interface toward dendrite of bi-layered separator, while a single blended membrane does not seem to be suitable for a practical use. Post-mortem pictures and SEM investigation have confirmed this result.

Keywords: Gel polymer electrolyte; Lithium cells; Dendrites; Bi-layer separator; Blended membrane

1. Introduction

The continuous increase in the portable device market, such as mobile phones, laptop computers, has lead to the search for new electrochemical systems enabling to safely deliver sufficient power for a long time. For reasons of toxicity, Ni–Cd batteries are no longer a contestant in the race to equip the devices of this century. Actually, among the emerging technology (Ni–MH; Li–ion) the Li–ion batteries are at the moment the most efficient systems to supply the required power and energy. Nevertheless, the use of graphite-based composite electrode (372 mAh g^{-1}) limits the expansion of their capacity needed in a near future. In order to replace graphite, lithium metal electrode (3860 mAh g^{-1}) has long been identified as a promising alternative, but the interest rapidly declined due to the possibility of short-circuit associated to the lithium dendritic growth at the lithium metal surface upon cycling [1]. To circumvent this issue, Armand et al. suggested the use of a dry solid polymer electrolyte consisting of poly(ethylene oxide) (PEO) and a lithium salt [2]. While efficient, considering its ability to lower the dendritic growth, this type of separator operates well only above the polymer melting temperature, typically $T = 90\,^{\circ}C$. One of the most promising technologies for a room temperature application seems to be the use of gel polymer electrolyte (GPE) [3]. Our group recently investigated two different GPE configurations [4]. A classical approach consists in blending two polymers in order to obtain a unique membrane [5]. This separator, denoted hereafter blended membrane (BM), is composed of PEO domains swollen by the liquid electrolyte and a poly(vinylidene fluorine-*co*-hexafluoropropylene) (PVdF–HFP) framework, which brings the mechanical strength. On the other hand, a separator consisting of the adjunction of two films, one based on PVdF–HFP and the other based on PEO, was realized. This separator is denoted hereafter bi-layer separator (BLS). In this case, once swollen by the liquid electrolyte the PEO film enables the realization of a good interface

* Corresponding author. Tel.: +33 491 637 137; fax: +33 491 637 111.
E-mail address: rb@up.univ-mrs.fr (R. Bouchet).

0378-7753/$ – see front matter © 2005 Elsevier B.V. All rights reserved.
doi:10.1016/j.jpowsour.2005.09.026

with the lithium, while the PVdF–HFP film is used as an electrolyte sponge. The physico-chemical properties of both GPE have previously been investigated and reported [4]. Whatever the binary electrolyte used, the fundamental technical and scientific question of the dendritic growth remains. The aim of this paper is to propose a way to quickly and easily evaluate the ability of a given electrolyte to prevent short-circuits. To reach this goal, quick galvanostatic polarization experiments on Li/GPE/Li symmetric cells, and long galvanostatic cycling experiments on real battery configuration were performed and compared. Post-mortem investigations have enabled us to validate our procedure and to propose a sketch of the dendritic growth in both studied GPE membranes.

2. Experimental

2.1. Membranes preparation

The blended membranes were prepared by gelling PVdF–HFP (Elf-Atochem, Kynarflex 2801 containing 12% of hexafluoropropylene units with $M_v = 3 \times 10^5$ g mol^{-1}) in highly purified acetone. PEO ($M_v = 4 \times 10^5$ g mol^{-1} from Aldrich) was solvated by acetonitrile. All products were used as received. Once homogeneous, the two gels were poured in a laboratory blender together with DBP (from Prolabo) according to the Bellcore process [6], and vigorously blended for 15 min. The optimal composition was previously found as being 3/7/10 (w/w) of PEO/PVdF–HFP/DBP, respectively. After evaporation of the solvents we obtained freestanding films about 50 μm thick.

For the BLS separator, 35 μm PVdF–HFP, SiO_2 and DBP-based membranes were made according to the Bellcore process using a 3/2/4 (w/w), respectively. PEO thin films were obtained by first mixing in acetonitrile high molecular weight PEO ($M_v = 4 \times 10^6$ g mol^{-1} from Aldrich) and DBP in a 1:1 (w/w) and then by casting the solution on a Mylar® sheet using a doctor blade apparatus gapped at 0.15 mm. After room temperature solvent removal, a 10 μm thick film was obtained and laminated on one side of a Bellcore's PVdF–HFP separator [7].

2.2. Symmetric cells and batteries assembly

To evaluate the behavior of the BM or BLS membranes under galvanostatic polarization, symmetric Li/GPE/Li cells have been prepared. The membranes were washed with ether to remove the DBP, dried and put into an Argon filled glove box to be impregnated with a solution of ethylene carbonate–propylene carbonate mixture (EC/PC 1:1, w/w) containing 1 M dissolved lithium salt $LiN(CF_3SO_2)_2$ (Lithium bis(TriFluoromethaneSulphonyl)Imide commercially known as LiTFSI). The electrolyte membrane was sandwiched between two lithium foils laminated on a copper grid used as current collector. A homemade polypropylene mask having a 2 cm^2 circular opening in its center was used to fix the active lithium surface area. Afterwards, the cells were sealed in hermetic coffee bags, and taken out of the glove box. Schematic drawings of the symmetric cells are given in inserts of Fig. 1.

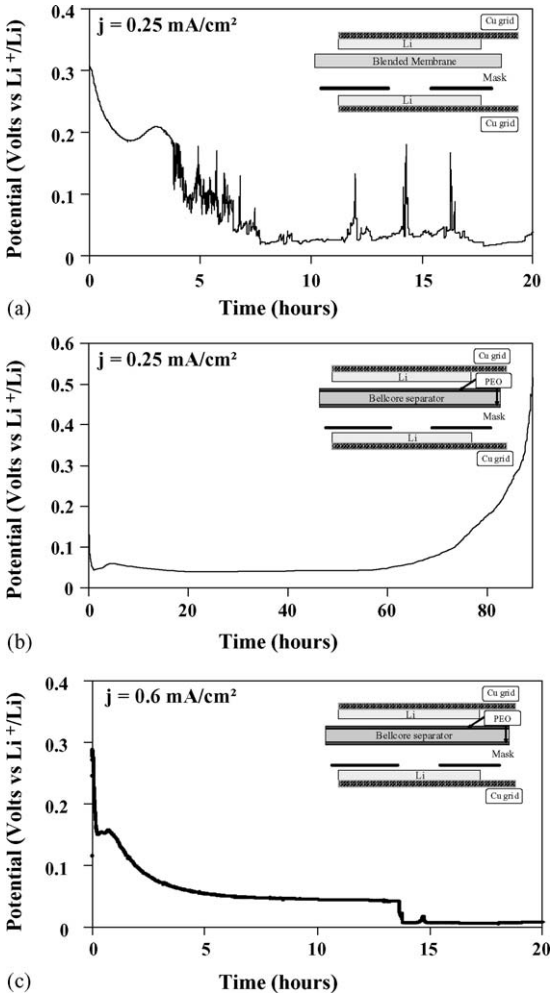

Fig. 1. Polarization curves of (a) a BM-based symmetric cells and (b) a BLS-based symmetric cell at $j = 0.25$ mA cm^{-2}. (c) Typical short-circuit observed on a BLS-based symmetric cell polarized at $j = 0.6$ mA cm^{-2}.

$Li_4Ti_5O_{12}$, provided by Telcordia technology, was used as a reference active material because of its high reversibility with regard to the lithium insertion/extraction [8]. Outside the glove box, 2 cm × 2 cm composite cathodes were prepared from a mixture of active material (56 wt.%), PVdF–HFP copolymer (15%), DBP (23%) and carbon black (6%) dissolved in acetone. The resulting slurry was spread onto a glass plate resulting in a 50 μm plastic film after solvent evaporation. Within these conditions, a $Li_4Ti_5O_{12}$ composite cathode having 3 mg of active material per square centimeter presents a capacity of about 0.5 mAh cm^{-2}. Cathodes were first laminated together with a pre-treated aluminum grid on one side. In the case of BLS-based batteries, a second lamination step was performed in order to stick the PVdF–HFP side of the membrane onto the positive electrode. Afterwards, once the DBP extracted by means of several washes into ether solutions, the half-cells were transferred into the glove box, where they were impregnated with liquid electrolyte. A lithium foil, pre-laminated on a copper grid, was then placed on top of the cathode/GPE half-cell to produce a battery. Finally, they were sealed in hermetic coffee bags, taken out of the glove

box, and cycled under different conditions without any external pressure applied.

2.3. Instrumentation

Simple galvanostatic polarizations were performed with a Solartron 1470 multi-potentiostat. Batteries cycling were realized using a Mac Pile system (Biologic, Claix, France) operating in a galvanostatic mode. Samples for microscopy investigations were cross-sectioned in an argon filled glove box, and placed in a movable airlock system preventing them from any air exposure while being transferred into the scanning electron microscope (SEM) chamber [9,10]. SEM observations were performed by means of a Philips XL-30 FEG.

3. Li/GPE/Li symmetric cells polarization

Typical room temperature galvanostatic polarization curves of Li/GPE/Li symmetric cells, applying a current density of $j = 0.25\ \mathrm{mA\,cm^{-2}}$, are presented in Fig. 1a and b. We observe a general important decrease in the polarization (by a factor between 5 and 7) during the first 8 h prior to reaching a steady low voltage value. It was shown that this behavior has to be correlated to the evolution of the lithium passive layers under current [4]. In the case of BM-based symmetric cells, the induced voltage noisily drops to zero after only a few hours. Such a phenomenon, known as "fuse effect", was already reported and correlated to the appearance of punctual short-circuits [10,11]. In contrast, the BLS-based cells exhibit a noise-free curve (Fig. 1b). Therefore, after about 60 h, the voltage starts to diverge and is multiplied by a factor 10 at 90 h polarization for which the lithium anode (100 μm thick) is almost completely oxidized. In order to observe a short-circuit with this type of membrane, the current density applied was increased up to $j = 1.2\ \mathrm{mA\,cm^{-2}}$. For example, under $0.6\ \mathrm{mA\,cm^{-2}}$ conditions, 13 h are needed to obtain a sharp and well visible short-circuit (Fig. 1c).

Considering the first potential drop as the time needed for a lithium dendrite to reach the opposite electrode, Rosso et al. have established an experimental correlation between the current density and the short-circuit time (denoted t_{sc} hereafter) [11,12]. The basic idea behind this relation lies in Chazalviel's early theoretical approach of the dendritic growth in binary electrolyte for a current density superior to the diffusion-limited current density (j_s). In particular, this model predicted a dendritic growth for times close to Sand time t_{sc} (where the cation concentration at the cathode reached zero) [13]. Rosso et al. have applied this model in the case of current density inferior to j_s, taking into account the local variation of current density. They demonstrated that in such case, by neglecting the dendritic growth time with regard to the dendritic apparition time, a pseudo Sand behavior is expected, i.e. the time of the first observed short-circuit is proportional to $1/j^2$. Thus, according to these models, for $j < j_s$ a constant of proportionality, α, can be defined. It has to be infinite in the case of ideal interface and would be finite in the case of interfaces with local current density heterogeneities. In fact, whatever reasons for which the Li/electrolyte interface is heterogeneous, the $t_{sc} \times j^2 = \alpha$ value can be considered as a figure of merit for a given binary electrolyte. The higher the α value is, the better the electrolyte in term of dendrite progression limitation is. A simple way to test this prediction consists in using a wide range of current densities, and observing the ability for the separator to "stop" or not the dendritic growth.

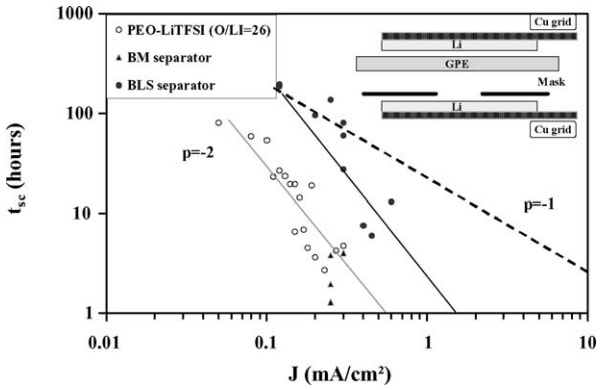

Fig. 2. Current density vs. short-circuit time for PEO–LiTFSI (O/Li = 26) separator measured at $T = 90\,^{\circ}\mathrm{C}$ [12], and for BM and BLS at $T = 20\,^{\circ}\mathrm{C}$. Dashed line represents the consumption of all the lithium foil.

Such a study was performed at 20 °C for cells based on both GPE, and the results are compared (Fig. 2) with the already reported values obtained for a solid polymer electrolyte (SPE) based on PEO–LiTFSI (O/Li = 26) and heated at $T = 90\,^{\circ}\mathrm{C}$ [12]. Beside a large distribution of the particular α values obtained for each cell, it appears a statistical tendency in agreement with the cited model. We found that the average α value of the BM-based cells, operating at room temperature, is in the same order as those of SPE at $T = 90\,^{\circ}\mathrm{C}$. On the contrary, a large improvement by almost one order of magnitude of α values was observed when using a BLS separator. For example, for $j < 0.3\ \mathrm{mA\,cm^{-2}}$, the total lithium foil (100 μm) consumption has systematically been obtained before any short-circuit appearance. This is stressed by the line shift that tends to indicate that, for a given capacity (and in order to prevent dendritic growth) the battery charge rate at 20 °C can be 10 times higher using BLS membranes than for the BM or SPE at 90 °C. Values and statistics are given in Table 1. Based on this methodology, a preliminary study of pulsed current charges effect, on the dendrites growth, was performed on BLS symmetric cells. Using a square wave profile with $j_{min} = 0$ and $j_{max} = 2\langle j \rangle$, first an average current density of $\langle j \rangle = 0.6\ \mathrm{mA\,cm^{-2}}$ was chosen and the impact of frequency checked on the range 0.05–500 Hz. Cells charged at a 0.5 Hz frequency have exhibited the highest t_{sc} values. As previously performed, a scan in current densities was then realized within this condition (Fig. 3). An average improvement by a factor 3 was found compare to the same

Table 1
Values of $t_{sc} \times j^2$ and number of cells investigated for the SPE, the BM and the BLS

	PEO–LiTFSI (O/Li = 26)	BM	BLS
$t_{sc} \times j^2$ ($\mathrm{h\,mA^2\,cm^{-4}}$)	0.33 (±0.12)	0.2 (±0.1)	3.3 (±2)
Number of studied cells	17	4	10

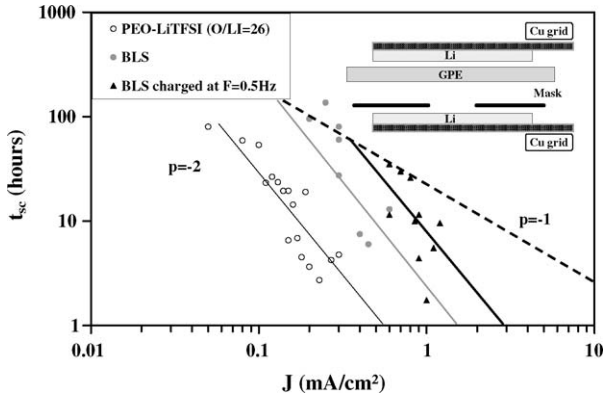

Fig. 3. Current density vs. short-circuit time for PEO–LiTFSI (O/Li = 26) separator measured at $T = 90\,^{\circ}C$ [12] (open circles), for BLS (closed circles) and for BLS charge with pulsed currents at $F = 0.5$ Hz (triangles) at $T = 20\,^{\circ}C$. Dashed line represents the consumption of all the lithium foil.

system polarized with continuous current. Such an encouraging results will now be confirmed in battery configuration, but it has been evidenced that the use of short-circuit time measurements has enabled to quickly define the optimal conditions to explore.

In short, the above observations have highlighted the difference between the two kinds of separators in term of time of dendritic short-circuit by means of simple galvanostatic polarization measurements on symmetrical lithium/GPE/lithium electrochemical cells. In order to validate this procedure as a "simulating method" to investigate the ability of a given electrolyte membrane to be a good physical separator with regard to the lithium dendritic growth, Li/$Li_4Ti_5O_{12}$ secondary batteries based on our GPE were investigated under galvanostatic cycling conditions.

4. Li/GPE/$Li_4Ti_5O_{12}$ batteries polarization

Li/GPE/$Li_4Ti_5O_{12}$ batteries were cycled at room temperature. A slow cycle is first realized to define the real capacity of

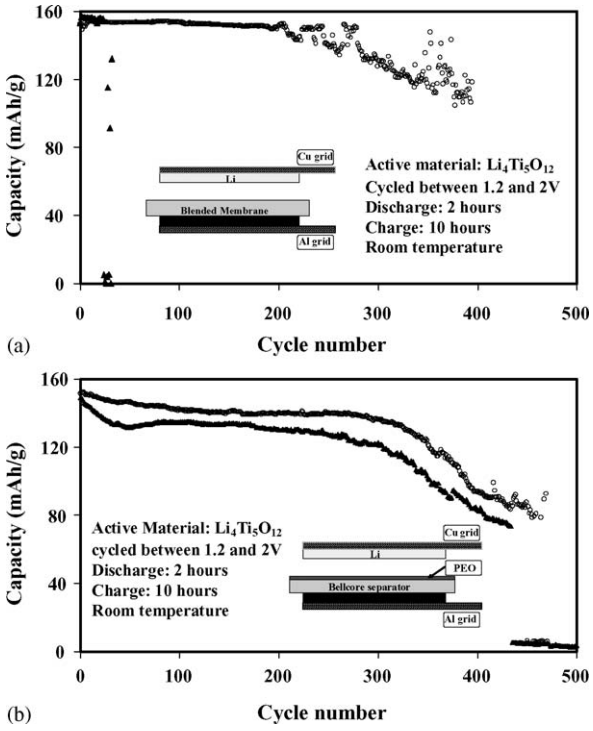

Fig. 4. D/2-C/10 galvanostatic cycling of batteries based on (a) BM and (b) BLS.

the positive electrode. Then, a full discharge and a charge at 2- and 10-h rates were applied in the 1.2–2 V range, respectively. This procedure corresponds to a charge at a current density of about $j = 0.05$ mA cm^{-2} for the lithium anode. For the BM-based samples, note that most of the accumulators have randomly been short-circuited after only a few cycles. The best and the worst results are presented in Fig. 4a. In the best case, after 200 steady cycles, fluctuations of the capacity retention start occurring. Such behavior was probably ascribed to the appearance of local and imperfect lithium dendritic short-circuits. On the contrary,

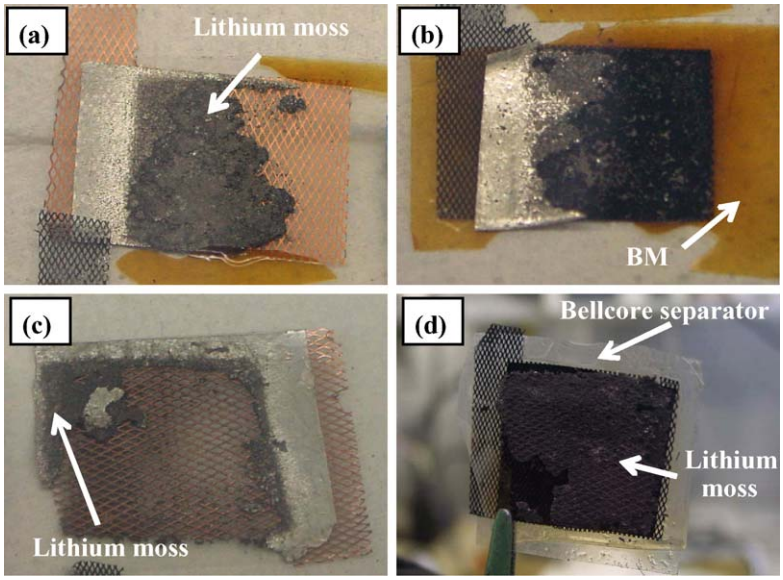

Fig. 5. Pictures of the lithium metal and the composite electrode for (a and b) BM and (c and d) BLS-based batteries, respectively.

Table 2
Average cycles number realized above 80% of the initial capacity and number of cells investigated for BM and BLS

	BM	BLS
Average cycle number	140 (±65)	320 (±20)
Number of studied cells	14	4

It is to note that 43% of the BM cells have performed less than 10 cycles. The presented statistic does not take these cells into account.

no BLS-based battery has presented short-circuit or random fluctuations (Fig. 4b). After an average of 320 cycles (see Table 2), the capacity retention starts to continuously decrease until dropping to zero. This phenomenon has recently been reported and linked to the conversion of all of the fresh lithium into highly passivated lithium "moss" (cf. Fig. 7). It allowed to provide an average lithium faradic efficiency estimated at 86% in good agreement with the values found in the literature [14]. Finally, a clear correlation between cyclability in real battery configuration and the $t_{sc} \times J^2 = \alpha$ value appears, i.e. batteries using BLS cycled almost one order of magnitude better than those using BM.

5. Post-mortem investigations

Dead batteries were dismantled in an Argon filled glove box. Anodes (Fig. 5a and c) and cathodes (Fig. 5b and d) were then photographed for macroscopic analysis. Furthermore, once cross-sectioned, the symmetric cells presented Fig. 1 were placed in a sample holder, previously described [9,10], and transferred into the SEM chamber without any air exposure (Figs. 6 and 7).

Although transparent before cycling the BM membrane then exhibits an orange coloration (Fig. 5a and b) that has been correlated to the degradation of the PVdF–HFP polymer in contact with lithium [15,16]. After such a long cycling, a part of lithium bulk is replaced by mossy lithium. For the region in contact with lithium moss, the BM membrane appears to be speckled all over its surface (Fig. 6a). Besides, some dendrite clusters remaining into the separator have also been observed (Fig. 6b). The presence of such holes can be ascribed to lithium electrodeposits penetration into the soft part of the composite membrane, thus demonstrating the incapacity for this membrane to efficiently stop the dendritic progression.

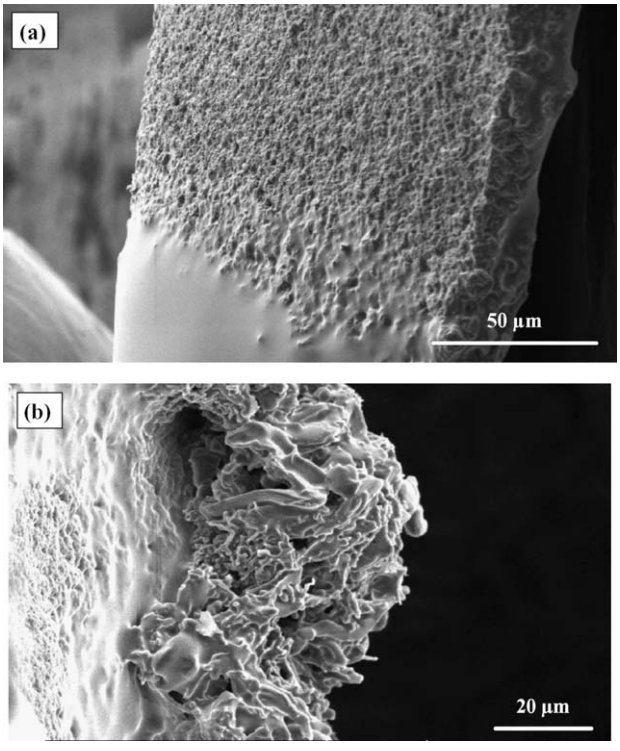

Fig. 6. (a) SEM picture of BM after cycling. (b) Typical SEM picture of deposited lithium aggregate stuck in a BM.

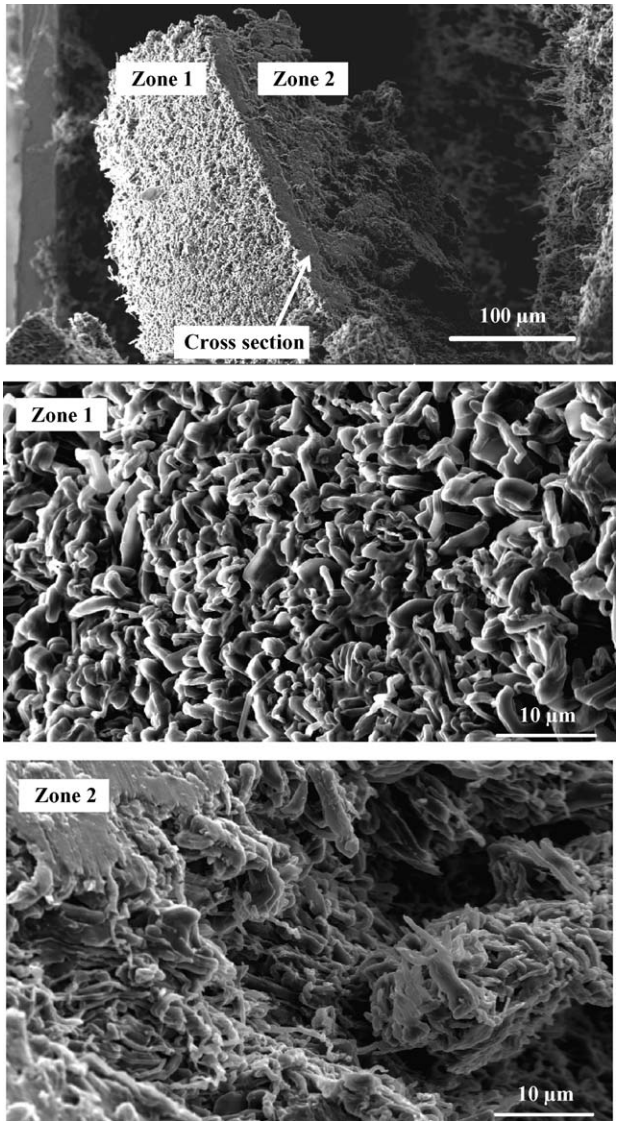

Fig. 7. SEM picture of the lithium deposit obtained by the use of a BLS. (a) Cross-section of a symmetric cell polarized until consumption of all the 100 µm lithium foil at $j = 0.25$ mA cm^{-2}. (b) Zoom of the Zone 1, corresponding to the area directly in contact with the BLS. (c) Zoom of the Zone 2, corresponding to the bulk of the lithium deposit.

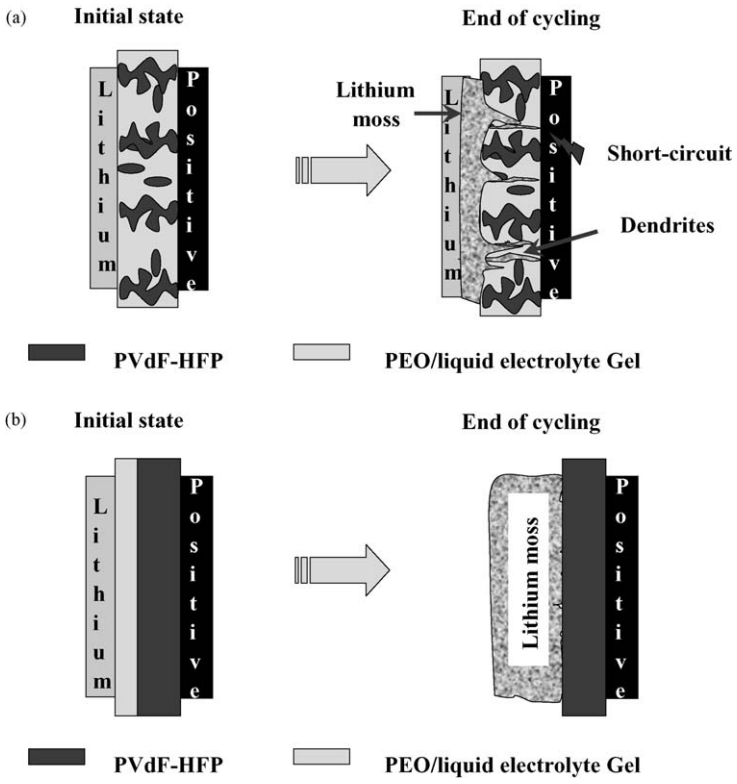

Fig. 8. Schematic explanation of the lithium deposition process in BM and BLS-based cells upon cycling.

On the opposite, BLS membrane remains colorless (Fig. 6d) confirming in the first place the role of chemical/electrochemical "buffer" played by the PEO film [17]. Furthermore, the plasticity of this layer, owing to its affinity with lithium, enables to maintain a good Li/separator contact throughout the cycling. In the BLS-based battery, we observed that the lithium foil was mostly converted into lithium moss (Fig. 5c), thus confirming the explanation given for the loss of capacity above 300 cycles [17,18]. This lithium moss can be considered as "dead lithium" because of its non-ability, as we have checked, to take an active part in the electrochemical reactions [14,18]. Fig. 7 shows the morphology of the lithium deposit (300 μm thick) resulting from the consumption of the 100 μm lithium foil. We are confident that the Li morphology was not affected by the process of cross-sectioning the cell. Zone 1 was in direct contact with the separator and was not modified by manipulation. The electro-deposit front is flat and regular, the density of the dendrites is high and their shape is curved as if their progression was stopped. Zone 2 is strongly indicative of mossy lithium with non-uniform growth. In this area, the electro-deposit seems to be more porous and the dendrites more needle-like as compared to Zone 1.

Explanation for the difference between both types of separator can be sketched as presented in Fig. 8. In the BM membrane, SEM pictures showed a co-continuous PEO/PVdF–HFP composite [4] in which 67% volume consists in a PEO/liquid electrolyte gel. It seems that this soft part of the composite membrane represents tunnels of progress (mean diameter about 2–5 μm) for electrodeposits, and therefore the BM cannot efficiently limit the dendritic growth. On the contrary, BLS presents two adjacent layers, one of which being a PEO gel ensuring a good interface and a good contact with the lithium electrode, and the other made out of a hard porous PVdF–HFP (mean diameter in the sub micron range) acting as a wall [19]. During the first cycles, lithium electrodeposition takes place without constraint in the soft layer and, it is believed that, reaching the PVdF-based separator, dendrites are stopped due to the hardness of this material compared to the PEO gel explaining the difference in density and in morphology observed in Zones 1 and 2 (Fig. 7).

6. Conclusions

Two different types of GPE have been investigated by means of galvanostatic polarization. Results providing Li/GPE/Li symmetric cells polarizations have given the same information as the cycling of $Li_4Ti_5O_{12}$/GPE/Li batteries but for a period 25 times lower. Furthermore, SEM investigations have confirmed the assumed failure processes based on both galvanostatic cycling of batteries (nearly 6 months) and simple galvanostatic polarization performed on symmetric lithium cells (about 1 week). Finally, these results demonstrate that t_{sc} measurements are a powerful tool to quickly check the ability for a membrane to stop the dendritic growth.

On another hand, the concept of a bi-layer separator membrane consisting of a polymer gel, ensuring a good interface with lithium metal, and a "hard" polymeric film, has shown a high ability to stop dendrites growth inside the separator at a current densities range commonly used in industrial batteries ($0.2 \leq j \leq 0.5\,mA\,cm^{-2}$). Operating at room temperature, this

separator is of prime interest in the race towards developing a safe lithium metal battery technology. BM membranes have exhibited poor physical separator properties to be efficiently used in accumulators. Nevertheless, whatever the separator used the problem of irregular lithium deposit formation remains and actions to alleviate this issue are being presently pursued in our group.

Acknowledgements

The authors are indebted to both the French Agency for Environment and Energy organization (ADEME) and the French Ministry of Research under a national team effort program named ALEP, for their strong support of this work.

References

[1] E. Peled, J. Electrochem. Soc. 126 (12) (1979) 2047.
[2] M. Armand, J.M. Chabagno, M.J. Duclot, in: P. Vashista, J.N. Mundy, G.K. Shenoy (Eds.), Fast Transport in Solids, North-Holland, New York, 1979, p. 131.
[3] J.M. Tarascon, M. Armand, Nature (London) 414 (6861) (2001) 359.
[4] L. Sannier, R. Bouchet, L. Santinacci, S. Grugeon, J.-M. Tarascon, J. Electrochem. Soc. 151 (6) (2004) A873.
[5] K. Nishimura, Polymer electrolyte and lithium polymer battery using the same, US 6,165,645 (2000).
[6] J.-M. Tarascon, A.S. Gozdz, C. Schmutz, F. Shokoohi, P.C. Warren, Solid State Ionics 86–88 (1) (1996) 49.
[7] L. Sannier, Accumulateur au lithium avec séparateur bi ou tri couche, FR 0207433 (2002).
[8] K. Zaghib, M. Simoneau, M. Armand, M. Gauthier, J. Power Sources 81–82 (1999) 300.
[9] F. Orsini, A. Du Pasquier, B. Beaudoin, J.M. Tarascon, M. Trentin, N. Langenhuizen, B.E. de, P. Notten, J. Power Sources 76 (1) (1998) 19.
[10] M. Dollé, L. Sannier, B. Beaudoin, M. Trentin, J.M. Tarascon, Electrochem. Solid State Lett. 5 (12) (2002) A286.
[11] C. Brissot, Ph.D. Thesis, Ecole Polytechnique, 1998.
[12] M. Rosso, T. Gobron, C. Brissot, J.-N. Chazalviel, S. Lascaud, J. Power Sources 97–98 (2001) 804.
[13] J.-N. Chazalviel, Phys. Rev. A 42 (1990) 7355.
[14] H. Ota, X.M. Wang, E. Yasukawa, J. Electrochem. Soc. 151 (2004) A427.
[15] H.S. Choe, J. Giaccai, M. Alamgir, K.M. Abraham, Electrochim. Acta 40 (13–14) (1995) 2289.
[16] Z. Yaqiu, M.W. Urban, Langmuir 15 (10) (1999) 3538.
[17] L. Sannier, R. Bouchet, S. Grugeon, E. Naudin, E. Vidal, J.-M. Tarascon, J. Power Sources 144 (1) (2005) 231.
[18] P.C. Howlett, D.R. MacFarlane, A.F. Hollenkamp, J. Power Sources 114 (2003) 277.
[19] A. Du Pasquier, P.C. Warren, D. Culver, A.S. Gozdz, G.G. Amatucci, J.-M. Tarascon, Solid State Ionics 135 (2000) 249.